Research Article

Phoenix dactylifera L. extract: antioxidant activity and its application for green biosynthesis of Ag nanoparticles as a recyclable nanocatalyst for 4-nitrophenol reduction

Mahsa Nanaei[1] · Mohammad Ali Nasseri[1] · Ali Allahresani[1] · Milad Kazemnejadi[1]

Abstract
In this study, antioxidant activity as well as preparation of silver nanoparticles (Ag NPs) were investigated by spathe of *Phoenix dactylifera* L. extracts. Excellent antiradical activity was found for the methanolic extract. Also, catalytic activity of the bio-synthesized Ag NPs was evaluated in the presence of DPPH. Ag nanoparticles were bio-synthesized through an environmental friendly and cost-effective method using aqueous solution of *P. dactylifera* L. extract. The bio-synthesized Ag NPs were characterized by different techniques including Fourier transform infrared spectroscopy, ultraviolet–visible spectroscopy, transmission electron microscopy, X-ray diffraction, energy-dispersive X-ray spectroscopy, and dynamic light scattering. Then, we focused on optimization of the reaction parameters including pH, $AgNO_3$ concentration, interaction time, temperature and mixing ratio on the bio-synthesis of Ag NPs according to surface plasmon band for Ag NPs around $\lambda = 425$ nm. Finally, catalytic ability of the NPs was investigated toward reduction of 4-nitrophenol in the presence of $NaBH_4$, as a model reaction, the results indicated excellent catalytic ability of the NPs for the reduction of 4-nitrophenol for short reaction time. The bio-synthesized Ag NPs demonstrated well recyclability toward 4-nitrophenol reduction without any significant reactivity loss. The recovered NPs were studied by some analytical and spectroscopic methods.

Keywords Silver nanoparticles · Spathe of *Phoenix dactylifera* L. extract · Antioxidant · 4-Nitrophenol reduction · Green catalyst

1 Introduction

In recent years, Ag nanoparticles have received a large volume of attention from scientists due to of their outstanding properties in various fields of application. Well conductivity, low toxicity, chemical stability and catalytic property are some intrinsic properties of Ag NPs [1]. These noble metal nanoparticles have unique biological activities such as antimicrobial, anti-viral, anti-fungal, anti-inflammatory, anti-bacterial, antiseptic, disinfectant, cancer diagnosis and treatment [2–4]. From this point of view, they can be incorporated into a variety of materials in order to nail a specific goal [5] such as topical cream, antiseptic sprays, wound dressing, pharmaceutical preparations, medical implant coatings etc. [6–11]. They are able to change the three-dimensional structure of proteins in microorganisms (viruses, bacteria and fungi) by interaction with their disulfide bonds (thiol groups) and subsequently block functional operation and inactivation of them [12]. Also, they are well known as a promising tools for the catalytic reduction of 4-nitrophenol in the presence of $NaBH_4$ [13–16].

As a result, due to continues demand for Ag NPs over the two recent decades, a wide range of physical and chemical methods have been developed for preparation of these nanoparticles [17]. Conventional chemical and

✉ Milad Kazemnejadi, miladkazemnejad@yahoo.com; miladkazemnejadi@birjand.ac.ir; Mahsa Nanaei, mahsa.nanaei@gmail.com; Mohammad Ali Nasseri, manaseri@birjand.ac.ir; Ali Allahresani, a_allahresani@birjand.ac.ir | [1]Department of Chemistry, Faculty of Sciences, University of Birjand, Birjand, Iran.

SN Applied Sciences (2019) 1:853 | https://doi.org/10.1007/s42452-019-0895-4

Received: 17 April 2019 / Accepted: 8 July 2019 / Published online: 13 July 2019

physical approaches for the synthesis of silver nanoparticles often involve expensive and toxic materials and solvents, using toxic reducing agents and stabilizers to prevent unwanted agglomeration of NPs and are non-environmentally friendly [18]. So, there is a widespread interest for finding a new green and reliable approach to synthesis of silver nanoparticles [19], that efficiently controls the shape, size, stability and physiochemical properties of NPs [20, 21].

In recent years, the use of plant extract has fascinated scientists for the preparation of Ag NPs. These interest arise from its eco-friendly, economical, rapid and non-pathogenic nature of this approach for the bio-synthesis of NPs through a simple single step, that is potentially advantageous over the previously reported chemical or physical methods. The plant extract plays a dual functions involves reduction and stabilization (capping) of the NPs [22]. There are a lot of reports to date on plant extract-mediated bio-synthesis of Ag NPs that some recent reported plant come as follow: *Ficus benghalensis* [23], *Aloevera* [24], *Talinum triangulare* [25], *Cressa Cretica* [26], *Azadirachta indica* [27], *onion* [28], *basil* [29], *Shikakai and Reetha* [30], *Tamarind fruit* [31], *Ipomoea asarifolia (Convolvulaceae)* [32], *Syzygium aromaticum* [33], *Radix Puerariae* [34], *Vaccinium macrocarpon* [35], and *alliandra haematocephala* [36].

Phenol and its derivatives are one of the most widely used compounds in the industry and due to its relative stability in the environment, the ability to dissolve in water, high toxicity and health problems, its removal from industrial wastewater is of great importance in protecting the environment. Silver nanoparticles are one of the most effective catalysts to reduces these compounds and subsequently remove them from wastewater. For this reason, the bio-synthesized Ag nanoparticles are a good option for the reduction of nitrophenol compounds. Several plants have been reported to catalyze this reaction using the bio-synthesized Ag nanoparticles [37–40].

Phoenix dactylifera L. (*P. dactylifera*) which belongs to the *Arecaceae* family, is widely cultivated in Middle East and America for nutritional values and is considered as one of the valuable source of natural medicinal products which acts against various diseases [41]. Therefore, this fruit is mainly used and have pharmacological properties such as anti-inflammatory, anti-microbial, angiogenesis, which used as astringent, vermicide, detersive, febrifuge and aphrodisiac in Persian traditional medicine [42]. It contains anthocyanins, tannins, phenolic acids, sterols, carotenoids, and flavonoids [43]. In addition, the spathe of *P. dactylifera* L. (which is called Tarooneh by Persian folk) contain steroids, triterpene steroids, oils and flavonoids and used as tranquilizer, sedative, nerve tonic and for rheumatoid arthritis [44].

Herein, we have reported the bio-synthesis of Ag NPs using the spathe extract of *P. dactylifera* L. as a reducing and capping agent. The reaction parameters including pH, temperature, interaction time, $AgNO_3$ and plant extract concentration and its mixing ratio were studied in this article. Then, the efficiency of the bio-synthesized Ag NPs was evaluated for the catalytic reduction of 4-nitrophenol using sodium borohydride at room temperature. Also, the antioxidant activity of the spathe extract of *P. dactylifera* L. was evaluated by DPPH assay.

2 Experimental

2.1 Plant and materials

Fresh spathe of the *P. dactylifera* L. was collected from Khozestan, Iran and were rinsed with deionized water, air-dried at room temperature and finely fine powdered and kept in a dark closed container. All the chemicals were of analytical reagent grade purchased from Sigma Aldrich and used as received without further purification.

2.2 Instruments

Electronic spectra were performed on a UV Spectrolab BEL photonics over the 200–900 nm wavelength range. FTIR spectra were recorded on a JASCO FT/IR 4600 instrument in the range of 450–4000 cm^{-1}. The crystal structure of the Ag NPs was studied by Bruker AXS D8-advance X-ray diffractometer using Cu-Kα radiation. TEM image of the bio-synthesized Ag NPs was obtained on a JEOL-2010 transmission electron microscope with an accelerating voltage of 200 kV. HRTEM image of the biosynthesized Ag NPs were obtained with a HR-TEM FEI TEC9G20 instrument with an accelerating voltage of 200 kV. Size distribution of NPs were measured by DLS analysis on a HORIBALB550 instrument. The NMR spectra (^1H and ^{13}C) were recorded DMSO-d_6 using a 300 MHz instrument. The Mass spectroscopy was performed on a Bruker autoflex speed mass spectrometer. EDX spectroscopy was recorded on a field emission scanning electron microscope (FESEM, JEOL 7600F), equipped with a spectrometer of energy dispersion of X-ray from Oxford instrument.

2.3 Synthesis of silver nanoparticles

Preparation of plant extract: 5 g of the plant powder was added to 100 mL of deionized water. The mixture was then mechanically stirred for 20 min in reflux conditions, then cool to room temperature and finally filtered through a Whatman No.1 filter paper. The filtrate immediately is used for the bio-synthesis of Ag NPs.

25 mL of aqueous solution of $AgNO_3$ (0.025 M) was added dropwise into 25 mL of spathe of *P. dactylifera* L. extract. The resultant mixture was mechanically stirred at 80 °C for 20 min. The silver nanoparticles were obtained by centrifugation of the mixture (5500 rpm) for 20 min followed by re-dispersion in deionized water in order to elimination of any uncoordinated biological molecules [45]. The Ag NPs were isolated by centrifugation followed by drying under vacuum at room temperature.

2.4 Catalytic reduction of 4-nitrophenol by Ag NPs

Briefly, in a 1 cm path length standard quartz cuvette, an aqueous solution of 0.01 M 4-nitro phenol (30 µl) was added to the 0.3 mL of the freshly prepared $NaBH_4$ (0.1 M). Then, 0.3 mL of aqueous solution of the bio-synthesized Ag NPs (dispersed in water) were added to the mixture. The resultant mixture was shaken and quickly placed to the UV–Vis instrument. Progress of the reaction was monitored spectrophotometrically by consecutive recording of UV–Vis spectra every minute in a scan range of 200–550 nm at ambient temperature.

For isolation and characterization of 4-aminophenol, in a typical run, 4-nitrophenol (1.0 mmol) and the freshly prepared $NaBH_4$ (2.0 mmol) were added to 5 mL of aqueous solution of the bio-synthesized Ag NPs (dispersed in water). Progress of the reduction was monitored by thin layer chromatography (TLC). Upon reaction completion, 10 mL EtOAc was added to the mixture and Ag NPs were separated by centrifugation. Then, the organic layer was separated and the aqueous layer was further extracted by 2× 10 mL EtOAc. The organic layers were combined and the solvent was removed under reduced pressure to give the crude 4-aminophenol. The product was recrystallized from ethanol to afforded pure 4-aminophenol (98% isolated yield). 4-aminophenol was characterized by ^{1}H NMR, ^{13}C NMR and Mass spectroscopy (Fig. 1a–c).

4-aminophenol: Reddish-yellow crystal, m.p 188 °C, ^{1}H NMR (300 MHz, DMSO-d_6): δ(ppm): 4.36 (s, 2H, NH_2), 6.40 (d, 2H, J = 6.5 Hz, C–H Ar), 6.47 (d, 2H, J = 6.5 Hz, C–H Ar), 8.23 (s, 1H, OH), ^{13}C NMR (75 MHz, DMSO–d_6): δ(ppm): 39.5, 115.2, 115.5, 140.7, 148.2. MS (m/e) = 109 [M^+].

2.5 Antioxidant activity of *P. dactylifera* L. extract

For antioxidant assays, a methanolic extract according to the following procedure was provided: in a test tube, 0.15 g of dried powder was added to 3 mL of 80% methanol. The resulting mixture was extracted by ultrasound for 45 min. The extract was placed in the dark for 15 min, after which it was centrifuged for 15 min (5000 rpm) and kept at 4 °C until the test was performed. Various concentrations (0.0008, 0.0016, 0.0032, 0.0064 mg/mL) of methanolic extract of *P. dactylifera* L. were prepared. DPPH solution was prepared by dissolution of 4.63 mg DPPH in 80% methanol (100 mL). Then, 75 µL of different concentrations of extract was mixed with 3.9 ml of DPPH and after storing the tubes for 30 min in darkness, their absorbance was read at 517 nm. Control includes DPPH and solvent. According to the calibration curve, antioxidant activity was calculated using the following formula (1):

$$\text{Inhibition (\%)} = \frac{Abs_{Control} - Abs_{Sample}}{Abs_{Control}} \times 100 \quad (1)$$

The results of the antioxidant activity of the extract was reported based on IC_{50} in mg/ml of the extract. IC_{50} is said to be a concentration in a extract, that could be quenched 50% of the free radicals in a reaction medium [46, 47].

3 Results and discussion

To find optimum conditions for the bio-synthesis of Ag NPs by aqueous extracts of spathe of *P. dactylifera* L., the reaction parameters were investigated. In this way, the effect of pH, interaction time, temperature, mixing ratio and extract concentration were studied. In all of the experiments, the formation of Ag NPs was monitored by recording UV–Vis spectra according to the surface plasmon resonance (SPR) around 450 nm (Fig. 2) [48].

3.1 Optimization of reaction parameters

The bio-synthesis of Ag NPs was performed at different pH in the presence of spathe of *P. dactylifera* L. extract. Figure 2a shows the absorption spectra of the resulting solution at the pHs of 4, 5, 6, 7, 8, 9 and 11. As shown in the Fig. 2a, increasing of pH from 4 to 11, increases the intense absorption at the corresponding wavelength (about 450 nm). This behavior could be attributed to the increase of colloidal silver nanoparticles and reduction rate [49]. It is well known that the particle size is expected to be larger in acidic medium than in basic, because, in basic medium, hydroxide ions charging the surface of NPs and thus maximum electrostatic repulsion occurs [50, 51]. Moreover, it is well known that, the position of the nanoparticles SPR peak will have shifted with varying the reaction conditions. This shift indicated that the nanoparticle size is altered [17, 44]. The results suggest that pH is one of the main and effective factors in the bio-synthesis of Ag nanoparticles. It was found that the pH 9 is ideal for the bio-synthesis of Ag NPs by *P. dactylifera* L. extract. Furthermore, the observed single absorption band proposed that the prepared particles are nearly spherical in shape; because deviation from

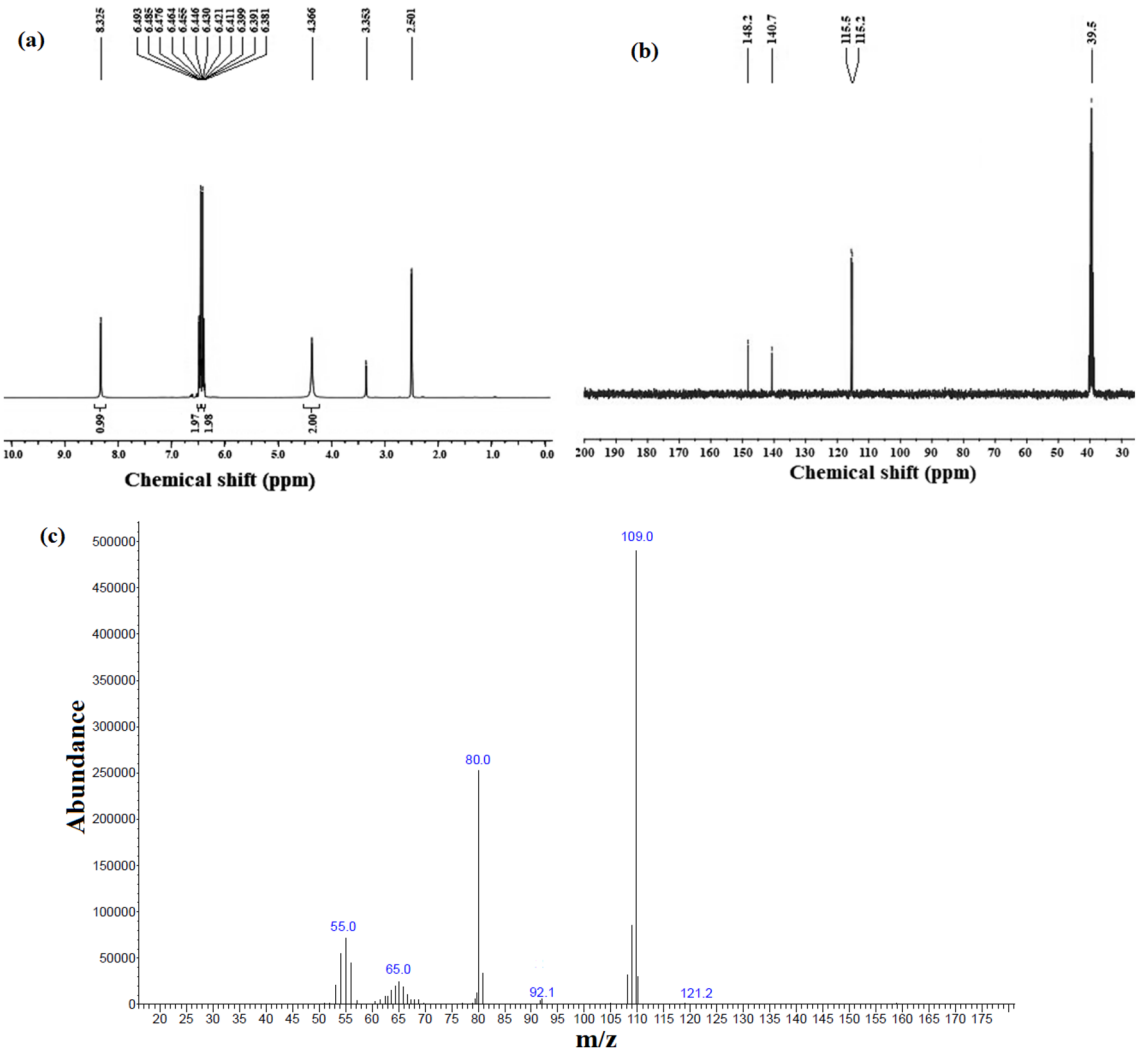

Fig. 1 **a** ^{1}H NMR, **b** ^{13}C NMR, and **c** mass spectra of 4-minophenol

spherical shape, provide another excess absorption band in the UV–Vis spectra in high pH values [21].

Various concentrations of $AgNO_3$ were tested in the synthesis of Ag NPs using spathe of *P. dactylifera* L. extract (Fig. 2b). The results indicated that the most absorption intensity correspond to Ag NPs was obtained with 25 mM aqueous solution of $AgNO_3$. Generally, with higher concentrations the absorption intensity decreases. As a result, didn't find any satisfactory results at lower concentrations.

Temperature also had an impressive impact on the absorption intensity of Ag NPs and the efficiency of them. As shown in Fig. 2c, the most SPR band intensity was observed at 40 °C. The intensity of SPR band decreases at higher or lower temperatures.

The effect of interaction time is also investigated on the synthesis of Ag NPs using aqueous extract of spathe of *P. dactylifera* L. extract (Fig. 2d). The electronic spectra were recorded at the time interval of 3, 15, 30, 45, 60 and 90 min while temperature and pH are kept constant at 40 °C and 9, respectively. The absorption band at λ ~ 450 nm correspond to SPR of Ag NPs, increased as a function of time during 90 min time interval. The results suggest that reduction of silver ions efficiently take place for 30 min. No change was detected in the SPR band intensity after more time of the reaction, which indicates the completion of the reduction of silver ions.

Due to direct relationship of ratio of the extract, as reducing and stabilizing agent, to size of Ag NPs, different mixing ratio of plant extract and silver salt were examined (different ionic strength of silver nitrate) [52]. A strong absorption bands were observed in all mixing ratios but the ratio of 1:3.5 (v/v) exhibited the highest intensity (Fig. 2e). No trend is observed at higher or lower ratios, but in general, the absorption intensity slowly decreased in higher mixing ratios (Fig. 2e). However, Dubey et al. also reported the decreasing trend in

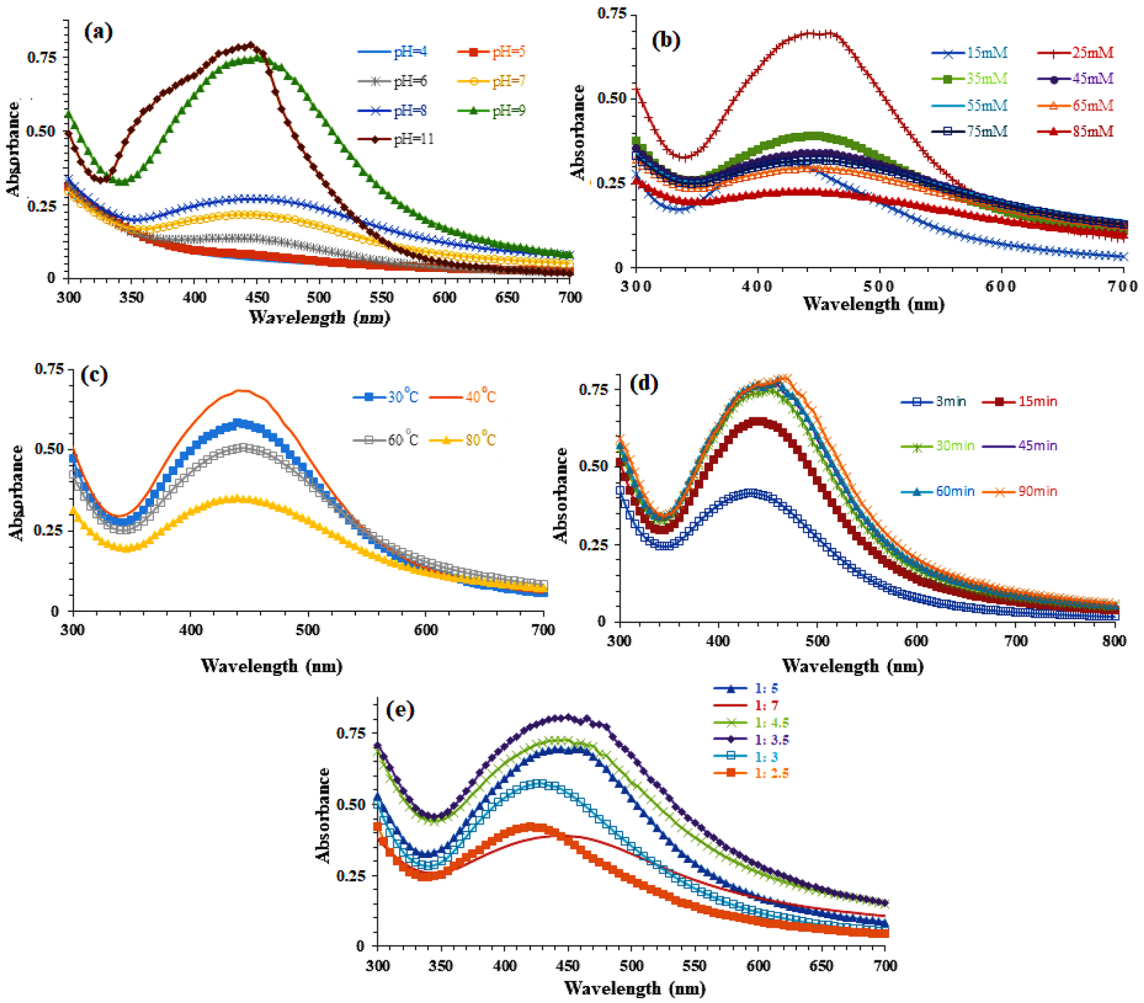

Fig. 2 UV–Vis spectra obtained from spathe of *Phoenix dactylifera* L. extract-mediated preparation of Ag NPs after at different: **a** pH values of the reaction mixture; **b** $AgNO_3$ concentration; **c** temperature; **d** interaction time intervals; and **e** plant extract: $AgNO_3$ mixing ratio

the formation of silver nanoparticles with the increase of silver ion concentration [20].

In the following, in order to achieve the complete reduction of silver ions, we investigated the effect of the plant extract concentration. The experiments were conducted in various concentration of the plant extract from 2 to 20% in 0.025 M silver nitrate solution. Various concentrations (2, 5, 10, 20%) of aqueous extract of *P. dactylifera* L. were prepared by boiling different amounts of the plant in deionized water (100 mL) for 20 min. The absorption spectra of Ag NPs were obtained with changing the concentration of plant extract at the optimized conditions, i.e., 40 °C, pH 9 for 30 min. The result indicated that 7% extract concentration give the highest possible absorption correspond to Ag NPs SPR band (Not shown in the Figure). With an enhancement in concentration of the plant extract, the peak intensity decreases.

3.2 Characterization of the bio-synthesized Ag NPs

The FTIR spectrum of the bio-synthesized Ag NPs was shown in Fig. 3. As shown in Fig. 3, the absorption bands at 1603 cm^{-1} and 1035 cm^{-1} were assigned to stretching vibration of C=C and C–O groups respectively [53]. A broad band at 3420 cm^{-1} may corresponds to the stretching vibration of O–H of alcohol and phenolic compounds [54]. The band at 1282 cm^{-1} is corresponds to the stretching vibration of amines (C–N). These absorptions are responsible for the bio-synthesis [55] of Ag NPs and show the presence of biomolecules in plant extract and consequently possible interactions between Ag and the bioactive molecules that could be efficiently bind to metal. In this way, the biomolecules play a role of capping, stabilization and reduction for NPs that retards their aggregation and leads to the stabilizing of silver nanoparticles [56].

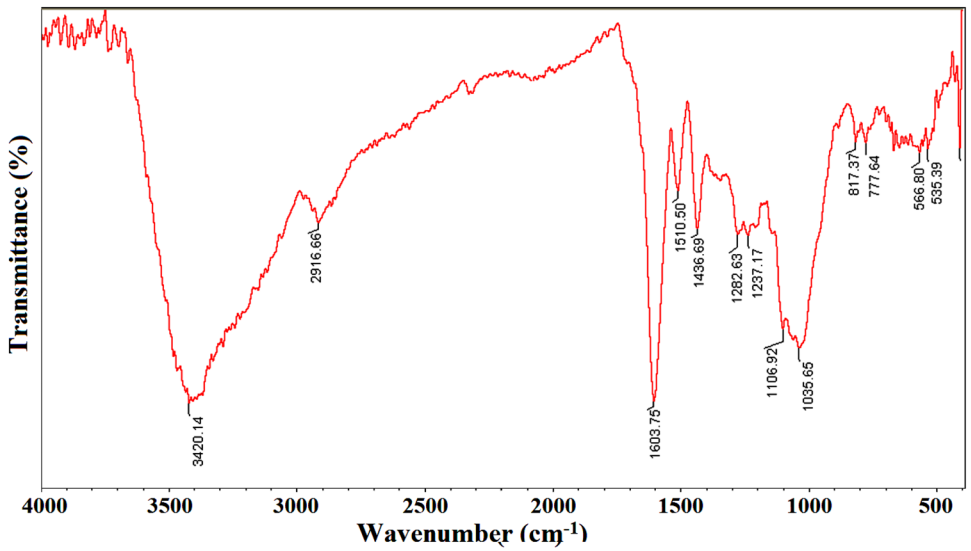

Fig. 3 FTIR spectrum of phyto-synthesized Ag NPs by spathe of *Phoenix dactylifera* L. extract

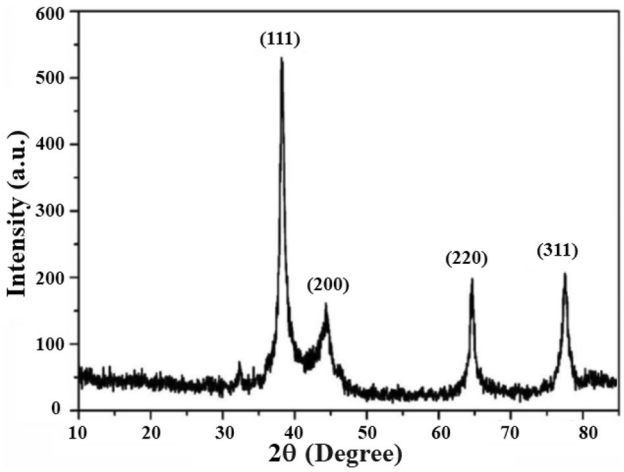

Fig. 4 XRD pattern of phyto-synthesized Ag NPs by spathe of *Phoenix dactylifera* L. extract

The bio-synthesized Ag NPs using spathe of *P. dactylifera* L. extract were characterized by X-ray powder diffraction in order to confirm their crystalline nature. As shown in Fig. 4 there are four main peaks in the XRD pattern of Ag NPs at 2θ = 38.17°, 44.17°, 63.52° and 78.32° correspond to the indices (111), (200), (220), and (311) respectively, which was completely in agreement with the facets of face centered cubic crystal structure of silver [57] and the reported standard of Joint Committee on Powder Diffraction Standards (JCPDS) file No. 84-0713.

TEM and HRTEM images from the bio-synthesized Ag NPs revealed that the particles are nearly spherical in morphology with the average size of 15 nm (Fig. 5a, c). The lattice fringe spacing indicated in the HRTEM image is 0.243 nm, which correspond to (111) plane of Ag NPs (Fig. 5c) [29, 57, 58]. Also, DLS analysis of the NPs proposed that size distribution of the particles was between 15 and 20 nm (Fig. 5b).

Preparation of Ag NPs was confirmed by the presence of Ag Lα and Ag Lβ peaks at about 3.0 keV and 3.2 keV respectively [50, 53, 58]. Other peaks represent C, O, N elements (totally about 33% wt), which belong to the extracted biomolecules (Fig. 5d). The values for the elements are shown in the inset table of Fig. 5d.

3.3 Catalytic reduction of 4-nitrophenol

Catalytic activity of the bio-synthesized Ag NPs was investigated using a model reaction, based on the reduction of 4-nitrobenzene in the presence of $NaBH_4$ in aqueous medium [22]. The reaction was conducted in a quartz cuvette cell of UV–Vis instrument. The reaction progress could be readily monitored by UV–Vis; because, when excess $NaBH_4$ was added to the substrate 4-nitrophenol, a red shift occurred due to the formation of 4-nitrophenolate ion and the color turned from colorless to yellowish with absorption band at ~ 400 nm; while 4-aminophenol (the product), is colorless without any chromophore in the aqueous solution with absorption peak about 300 nm (Scheme 1). Moreover, phenolate ion that is formed by the treatment of $NaBH_4$ with 4-nitrophenol caused shift of the absorption peak at about 318–400 nm, which promoted spectrophotometric sensitivity of the method that can be monitored by a simple UV–Vis spectrophotometer (Scheme 1). The reaction is kinetically not favorable, but thermodynamically favorable with activation energy ~ 44 kJ mol^{-1} [22, 58].

It was proved that both substrate and reductant could be adsorbed on Ag NPs to electron transfer take place [1, 59]. Thus, with progress of the reaction, the absorbance of 4-nitrophenol (λ_{max} ~ 410 nm) is reduced and at the same

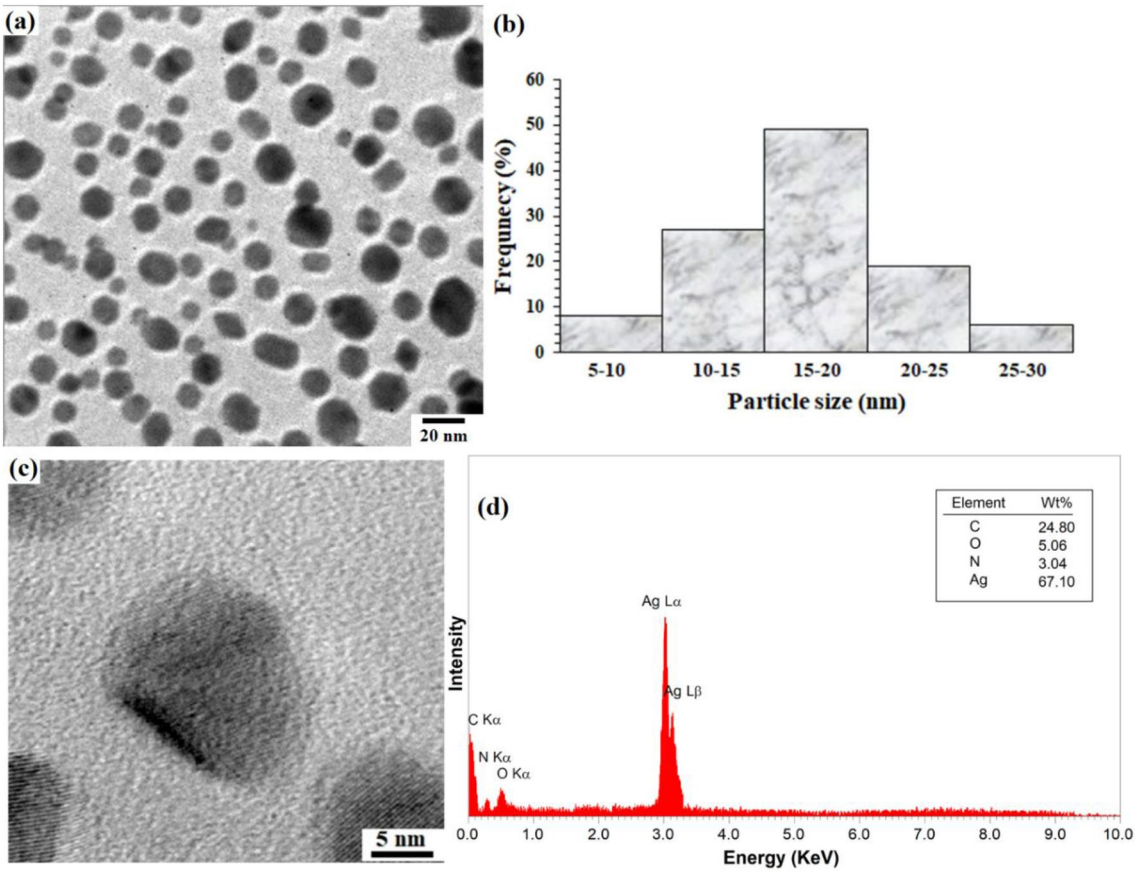

Fig. 5 **a** TEM image, **b** their size distribution determined by DLS analysis, **c** HRTEM image, and **d** EDX analysis of the phyto-synthesized Ag NPs by spathe of *Phoenix dactylifera* L. extract

Scheme 1 Representation of reduction of 4-nitrophenol catalyzed by the bio-synthesized Ag NPs

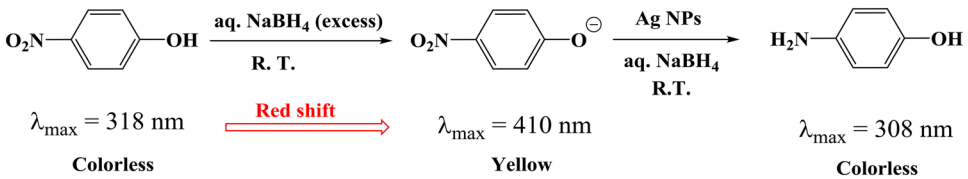

time the absorbance of 4-aminophenol (λ_{max} = 308 nm) developed with time. So, this model reaction allows the efficiently monitoring of 4-nitrophenol reduction as well as its kinetics spectrophotometrically. Figure 6a showing the catalytic activity of the bio-synthesized Ag NPs towards 4-nirophenol reduction. Reduction of 4-nitrophenol start after 40 min (induction time) of addition of $NaBH_4$. This time period is due to the required diffusion time in order to adsorption of 4-nitrophenol onto the Ag NPs surface, then the reduction take place [60]. The reduction was proceeds after the reduction time at t_0 = 40 min. Complete conversion takes place in 7 min. From Fig. 6a, it was obvious that the absorbance of the new peak with center of 300 nm, correspond to 4-aminophenol [59, 60], increases with increase in time, completely confirmed the activity of the bio-synthesized Ag NPs as a catalyst for the reduction of 4-nitrophenol. Furthermore, the reaction in absence of the Ag NPs didn't proceed and the color of the mixture remains yellow. Also, the absorption spectra didn't change with addition of freshly prepared $NaBH_4$ (0.1 M) even after 2 days in absence of the catalyst. A new peak appeared at ~ 390 nm shows the silver plasmon referring to the intermediate stage of the reduction, which is covered by 4-nitrophenol absorption band and was not visible before its complete reduction [14].

Because the reaction was performed under an excess amount of $NaBH_4$, thus its concentration could be considered as constant, and consequently the kinetics can be described by a quasi-first order rate law [22, 58]. With recording the absorption of 4-nitrophenol at different

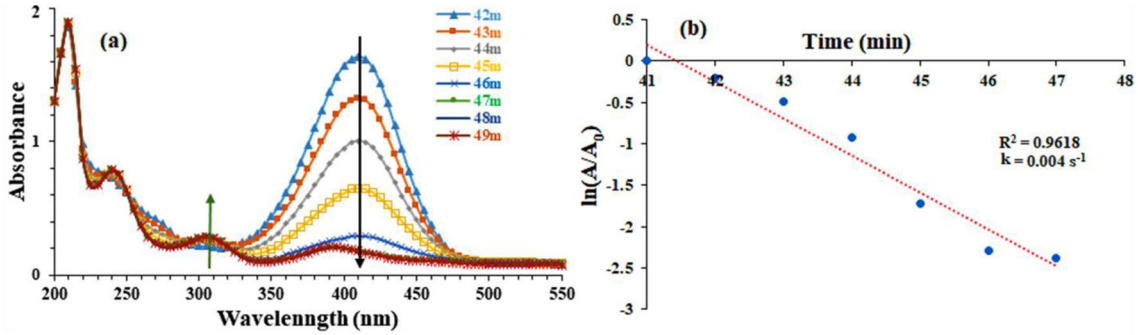

Fig. 6 **a** Successive UV–Vis absorption spectra for the reduction of 4-nitrophenol to 4-aminophenol acquired after $t_0 = 40$ min of addition of $NaBH_4$. The UV–Vis spectrum was recorded every minute until full conversion. For more clarity, the recorded spectra before t_0 were removed. Reaction conditions: 4-Nitrophenol aqueous solution (1.2×10^{-3} M), aqueous $NaBH_4$ (0.1 M, 50 µL), aqueous Ag NPs (0.3 mL), 25 °C. With progress of the reduction, the main peak at 410 nm correspond to nitrophenolate ions (black arrow) decreases, and consequently, the second peak at 308 nm, related to the product aminophenol, gradually increases (green arrow). **b** Plot of ln[A] versus time for the reduction of 4-NP introduced after 40 min of the introduction of $NaBH_4$ of variable concentrations

time intervals after an induction time $t_0 = 40$ min (in which no reduction takes place) at ~ 408 nm, the catalytic rate constant (k) for the reduction reaction can be defined by Eq. (2) [60]:

$$\ln\left(\frac{A}{A_0}\right) = -kt \tag{2}$$

where A_0 is the initial absorbance of 4-nitrophenol, A is the absorption of 4-nitrophenol at time *t* (sec.) and k is constant. Figure 6b demonstrates kinetic curve for the reduction of 4-nitrophenol as decreasing absorbance at wavelength of 408 nm. The value of 0.004 s^{-1} for the rate constant was measured by Eq. (2).

According to Langmuir–Hinshelwood mechanism for a heterogeneous catalyzed reduction, firstly, borohydride ions are adsorbed on the surface of Ag NPs and give them electrons [58]. This is induction period that takes place before any reduction. Then, 4-nitrophenol molecules adsorbed on Ag NPs surface by this electron and reduction take place. After reduction, the product 4-aminophenol is desorbed from the Ag surface and Ag NPs regenerated for the next cycle. Scheme 2 represent the plausible reaction mechanism for the reduction of 4-nitrophenol catalyzed by the bio-synthesized Ag NPs.

To show the recyclability of the bio-synthesized Ag NPs for the reduction reaction of 4-nitrophenol to 4-aminophenol, the recovered NPs were used for seven consecutive runs. In each cycle, the NPs were separated by centrifugation followed by washing with deionized water (2×20 mL). Figure 7 shows the results for recyclability of the Ag NPs, which an insignificant loss in efficiency was observed until 7th run. These results suggest that the bio-synthesized Ag NPs are stable during the reduction reaction and preserve their catalytic activity

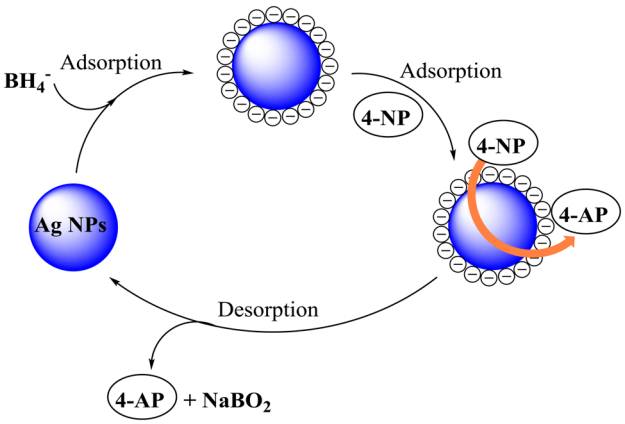

Scheme 2 Catalytic reduction of 4-nitrophenol by the bio-synthesized Ag NPs

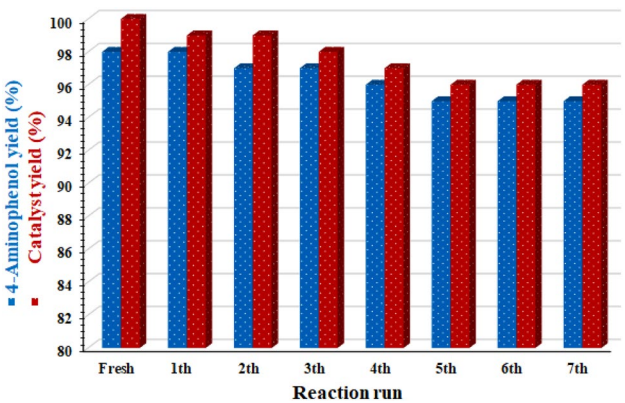

Fig. 7 Recyclability of the bio-synthesized Ag NPs over the reduction reaction of 4-nitrophenol to 4-aminophenol

for long tme. Furthermore, the recovered Ag NPs after 7th run, was studied by the analytical and spectroscopic methods. The FTIR spectra of the recovered NPs confirmed their structure (Fig. 8a). There is not found any agglomeration in the nanoparticles and/or deviation from shape as shown in the TEM image of the recovered NPs (Fig. 8b). Also, the size distribution of the NPs is as same as the corresponding fresh catalyst with mean size of 16.6 nm (Fig. 8c). Finally, the crystal structure of the NPs remains intact during reactions with four characteristic peaks at $2\theta = 38.17°$, 44.17°, 63.52° and 78.32° correspond to the indices (111), (200), (220), and (311) respectively (Fig. 8d).

Finally, to show uniqueness and advantage of the bio-synthesized Ag NPs by *P. dactylifera* L. extract, its catalytic performance was compared with those reported for 4-NP reduction using plant-mediated Ag NPs. The results were summarized in Table 1, which the reasonable size, low concentration of $NaBH_4$, recoverability for several times, low amount of Ag NPs, homogeneous morphology are some advantages of the catalytic activity of *P. dactylifera* L. over the most of the plants (Table 1).

3.4 Antiradical activity of *P. dactylifera L.* extract

Antiradical activity of the *P. dactylifera* L. extract was determined by DPPH assay. DPPH is a stable free radical with a single electron on N atom. Its methanolic solution is purple with a absorption at $\lambda_{max} = 515–520$ nm. DPPH could be reduced in the presence of an antioxidant, in which the maximum absorption undergoes a red shift to 400 nm (Scheme 3). Therefore, by measuring the reduction in the absorption intensity by a spectrophotometer, one can find the antioxidant properties of the extract. Figure 9 shows the antioxidant activity of the extract as a function of extract concentration as IC_{50} (mg/mL). An excellent antiradical activity was observed for the extract, which most of the DPPH radicals were quenched at 0.0064 mg/mL extract concentration (Fig. 9). The results demonstrated a linear relationship between the inhibition percentage and extract concentration in agreement with the literature [64]. This small IC_{50} reflects the high antiradical activity, which can be attributed to the presence of high levels of phenols and flavonoids in the extract [65].

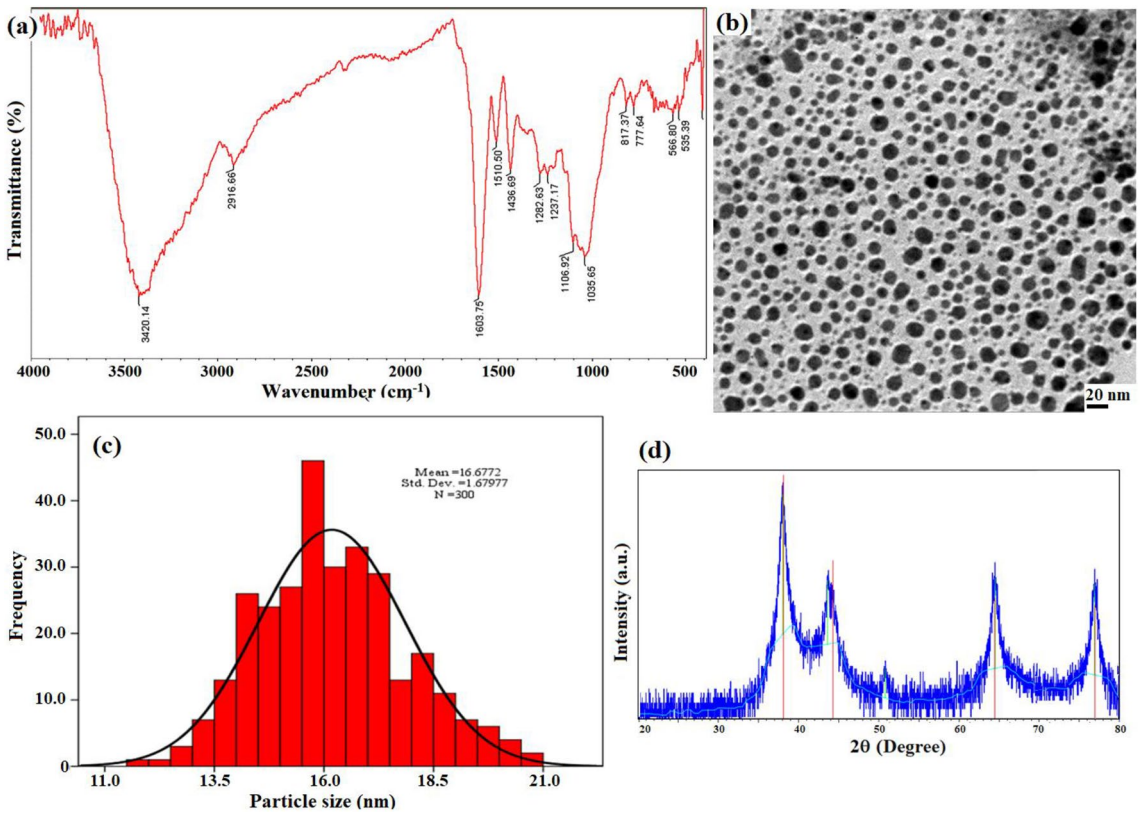

Fig. 8 **a** FTIR spectrum, **b** TEM image, **c** DLS analysis, and **d** XRD pattern of the recovered bio-synthesised Ag NPs after seven consecutive recycling for the reduction reaction of 4-nitrophenol to 4-aminophenol

Table 1 Comparison of the catalytic performance of Ag-NPs prepared by *Phoenix dactylifera* L. extract with previously reported plants for reduction of 4-nitrophenol

Plant	Type (amount)	Size (nm)	Shape and morphology	[$NaBH_4$]	Time (min)	Recoverability	References
Cerasus serrulata	Ag-NPs (NA)	10–50	Spherical	0.1 M	NA	–	[37]
Punica granatum	Ag-NPs (NA)	30	Spherical	1 mM	NA	–	[38]
Lotus Garcinii	Ag/RGO/Fe_3O_4 (5.0 mg)	40	Spherical	0.25 M	3	+	[39]
Lotus Garcinii	Ag-NPs (5.0 mg)	7–20	Spherical	0.25 M	17	–	[39]
Coleus forskohlii	Ag-NPs (25 µL)	30–50	Spherical	0.5 mM	30	–	[40]
Cylindrocladium floridanum	Mycogenic Ag NPs ($4.6–27.8\times10^{-4}$ mol/dm^3)	25	Spherical	6.6 mM	NA	–	[61]
Hamamelis virginiana	Ag NPs/perlite (12 mg)	8–25	Sheet	0.25 M	4	+	[62]
Thymbra spicata	Ag NPs (2.0 mg)	7	Spherical	0.25 M	1	+	[63]
Phoenix dactylifera L.	Ag NPs (0.3 mL)	15–20	Spherical	0.1 M	7	+	This work

RGO reduced graphene oxide

Scheme 3 Reduction of 2,2-diphenyl-1-picrylhydrazyl using plant extract

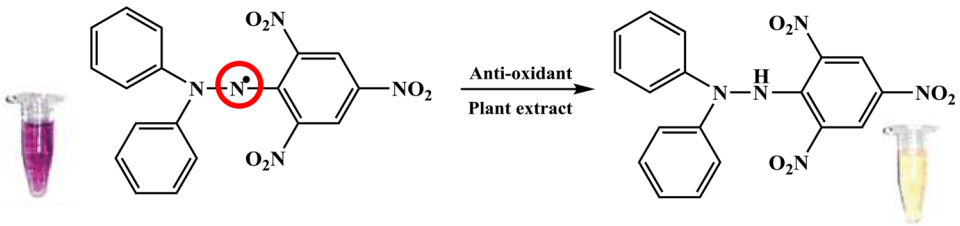

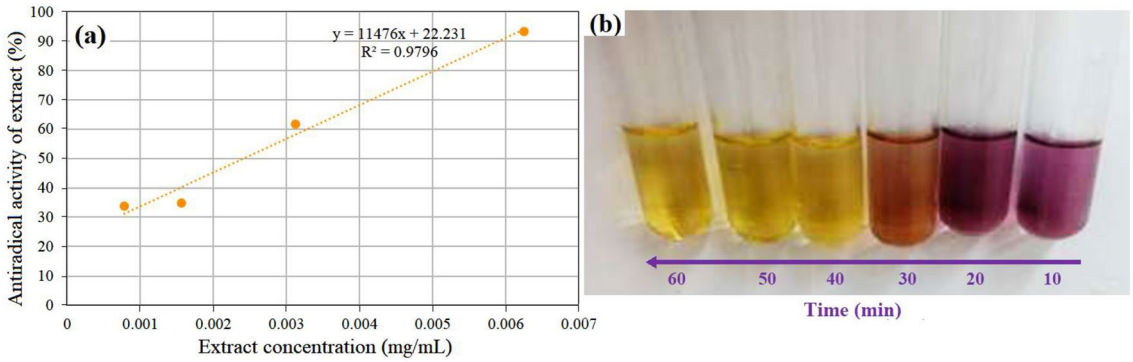

Fig. 9 **a** Linear relationship between inhibition percentage of the extract and extract concentration (mg/mL). **b** Interaction of *Phoenix dactylifera* L. extract on DPPH solution versus time

4 Conclusions

In this study we have reported a simple, fast and eco-friendly green process for the bio-synthesis of Ag NPs using aqueous solution of spathe *of P. dactylifera* L. extract in mild conditions. The silver nanoparticles were characterized with some techniques. The average size of the nanoparticles was obtained approximately 15–20 nm. The highest possible efficiency of the preparation of the Ag NPs were obtained in pH 9 at 40 °C for 30 min with mixing ratio of extract: Ag^+ of 1: 3.5 in the presence of 25 mM $AgNO_3$. The results demonstrated that the plant extract not only act as stabilizers, but also modified the size of the bio-synthesized NPs, which nearly homogeneous in size were obtained for the Ag NPs. Ag NPs were shown high catalytic activity towards reduction of 4-nitrophenol to 4-aminophenol in a short reaction time. The bio-synthesized Ag NPs could be readily recycled from the reaction mixture and

used as several consecutive runs while retaining its catalytic activity. The method suggests efficient alternative method for the bio-synthesis of nanoparticles to the previously reported chemical and physical methods. The methanolic extract of the plant demonstrated high level of antioxidant activity and suggests that it could potentially be used as an additive in medicines and nutrients.

Acknowledgements Authors gratefully acknowledge the financial support of this work by the Research Council of University of Birjand.

Compliance with ethical standards

Conflict of interest The authors declare that they have no conflict of interest.

References

1. Nasseri M, Behravesh S, Allahresani A, Kazemnejadi M (2019) Org Chem Res 5:190–201. https://doi.org/10.22036/org.chem.2019.160677.1185
2. Sun Y, Yin Y, Mayers BT, Herricks T, Xia Y (2002) Chem Mater 14:47364745. https://doi.org/10.1021/cm020587b
3. Yin B, Ma H, Wang S, Chen S (2003) J Phys Chem B 107:8898–8904. https://doi.org/10.1021/jp0349031
4. Smith AM, Duan H, Rhyner MN, Ruan G, Nie S (2006) Phys Chem Chem Phys 8:3895–3903. https://doi.org/10.1039/B606572B
5. Dimitrijevic NM, Bartels DM, Jonah CD, Takahashi K, Rajh T (2001) J Phys Chem B 105:954–959. https://doi.org/10.1021/jp0028296
6. Das TK, Ganguly S, Bhawal P, Remanan S, Mondal S, Das NC (2018) Appl Nanosci 8:173–186. https://doi.org/10.1007/s13204-018-0658-3
7. Callegari A, Tonti D, Chergui M (2003) Nano Lett 3:1565–1568. https://doi.org/10.1021/nl034757a
8. Ahmad A, Mukherjee P, Senapati S, Mandal D, Khan DI, Kumar R, Sastry M (2003) Colloids Surf B Biointerfaces 28:313–318. https://doi.org/10.1016/S0927-7765(02)00174-1
9. Vanaja M, Gnanajobitha G, Paulkumar K, Rajeshkumar S, Malarkodi C, Annadurai G (2013) J Nanostruct Chem 3:17. https://doi.org/10.1186/2193-8865-3-17
10. Song JY, Kim BS (2009) Bioprocess Biosyst Eng 32:79–84. https://doi.org/10.1007/s00449-008-0224-6
11. Yesilot S, Aydin C (2019) East J Med 24:111–116. https://doi.org/10.5505/ejm.2019.66487
12. Zhang L, Shen YH, Xie AJ, Li SK, Jin BK, Zhang QF (2006) J Phys Chem B 110:6615–6620. https://doi.org/10.1021/jp0570216
13. Du Y, Chen HL, Chen RZ, Xu NP (2004) Appl Catal A Gen 277:259–264. https://doi.org/10.1016/j.apcata.2004.09.018
14. Pradhan N, Pal A, Pal T (2002) Colloids Surf A Physicochem Eng Asp 196:247–257. https://doi.org/10.1016/S0927-7757(01)01040-8
15. Praharaj S, Nath S, Ghosh SK, Kundu S, Pal T (2004) Langmuir 20:9889–9892. https://doi.org/10.1021/la0486281
16. Hayakawa K, Yoshimura T, Esumi K (2003) Langmuir 19:5517–5521. https://doi.org/10.1021/la034339l
17. Swami P, Selvakannan R, Pasricha R, Sastry M (2004) J Phys Chem B 108:19269–19275. https://doi.org/10.1021/jp0465581
18. He R, Chian X, Yin J, Zhu Z (2002) J Mater Chem 12:3783–3786. https://doi.org/10.1039/B205214H
19. Dubey SP, Lahtinen M, Sarkka H, Sillanpaa M (2010) Colloids Surf B Biointerfaces 80:26–33. https://doi.org/10.1016/j.colsurfb.2010.05.024
20. Link S, El-Sayed MA (2000) Int Rev Phys Chem 19:409–453. https://doi.org/10.1080/01442350050034180
21. Mulvaney P (1996) Langmuir 12:788–800. https://doi.org/10.1021/la9502711
22. Aditya T, Pal A, Pal T (2015) Chem Commun 51:9410–9431. https://doi.org/10.1039/C5CC01131K
23. Saxena A, Tripathi RM, Zafar F, Singh P (2012) Mater Lett 67:91–94. https://doi.org/10.1016/j.matlet.2011.09.038
24. Chandran SP, Chaudhary M, Pasricha R, Ahmad A, Sastry M (2006) Biotechnol Prog 22:577–583. https://doi.org/10.1021/bp0501423
25. Ojo OA, Oyinloye BE, Ojo AB, Afolabi OB, Peters OA, Olaiya O, Fadaka A, Jonathan J, Osunlana O (2017) J Bionanosci 11:292–296. https://doi.org/10.1166/jbns.2017.1452
26. Vijayalakshmi M, Akilandeswari K, Kavitha K, Gokila S, Vinothkumar R (2018) Chem. Lett. 1:12–18. https://doi.org/10.26524/cl1813
27. Shankar SS, Rai A, Ahmad A, Sastry M (2004) J Colloid Interface Sci 275:496–502. https://doi.org/10.1016/j.jcis.2004.03.003
28. Saxena A, Tripathi RM, Singh RP (2010) Dig J Nanomater Bios 5:427–432
29. Ahmad N, Sharma S, Alam MK, Singh VN, Shamsi SF, Mehta BR, Fatma A (2010) Colloids Surf B Biointerfaces 81:81–86. https://doi.org/10.1016/j.colsurfb.2010.06.029
30. Sur UK, Ankamwar B, Karmakar S, Halder A, Das P (2018) Mater Today Proc 5:2321–2329. https://doi.org/10.1016/j.matpr.2017.09.236
31. Jayaprakash N, Vijaya JJ, Kaviyarasu K, Kombaiah K, Kennedy LJ, Ramalingam RJ, Munusamy MA, Al-Lohedan HA (2017) J Photochem Photobiol B Biol 169:178–185. https://doi.org/10.1016/j.jphotobiol.2017.03.013
32. Khaled JM, Alharbi NS, Kadaikunnan S, Alobaidi AS, Al-Anbr MN, Gopinath K, Aurmugam A, Govindarajan M, Benelli G (2017) J Clust Sci 28:3009–3019. https://doi.org/10.1007/s10876-017-1271-4
33. Venugopal K, Rather HA, Rajagopal K, Shanthi MP, Sheriff K, Illiyas M, Rather RA, Manikandan E, Uvarajan S, Bhaskar M, Maaza M (2017) J Photochem Photobiol B Biol 167:282–289. https://doi.org/10.1016/j.jphotobiol.2016.12.013
34. Balwe SG, Shinde VV, Rokade AA, Park SS, Jeong YT (2017) Catal Commun 9:121–126. https://doi.org/10.1016/j.catcom.2017.06.006
35. Khodadadi B, Bordbar M, Yeganeh-Faal A, Nasrollahzadeh M (2017) J Alloys Compd 719:82–88. https://doi.org/10.1016/j.jallcom.2017.05.135
36. Raja S, Ramesh V, Thivaharan V (2017) Arab J Chem 10:253–261. https://doi.org/10.1016/j.arabjc.2015.06.023
37. Karthik R, Hou YS, Chen SM, Elangovan A, Ganesan M, Muthukrishnan P (2016) J Ind Eng Chem 37:330–339. https://doi.org/10.1016/j.jiec.2016.03.044
38. Edison TJI, Sethuraman MG (2013) Spectrochim Acta Part A 104:262–264. https://doi.org/10.1016/j.saa.2012.11.084
39. Maham M, Nasrollahzadeh M, Sajadi SM, Nekoei M (2017) J Colloid Interface Sci 497:33–42. https://doi.org/10.1016/j.jcis.2017.02.064
40. Naraginti S, Sivakumar A (2014) Spectrochim Acta Part A 128:357–362. https://doi.org/10.1016/j.saa.2014.02.083
41. Yaish MW, Patankar HV, Assaha DV, Zheng Y, Al-Yahyai R, Sunkar R (2017) BMC Genom 18:246–263. https://doi.org/10.1186/s12864-017-3633-6
42. Ambigaipalan P, Shahidi F (2015) J Agric Food Chem 63:864–871. https://doi.org/10.1021/jf505327b

43. Kchaou W, Abbès F, Mansour RB, Blecker C, Attia H, Besbes S (2016) Food Chem 194:1048–1055. https://doi.org/10.1016/j.foodchem.2015.08.120
44. Hamedi A, Mohagheghzadeh A, Rivaz S (2013) Pharmacognosy J. 5:83–86. https://doi.org/10.1016/j.phcgj.2013.02.005
45. Rónavári A, Kovács D, Igaz N, Vágvölgyi C, Boros IM, Kónya Z, Pfeiffer I, Kiricsi M (2017) Int. J. Nanomedicine 12:871–883. https://doi.org/10.2147/IJN.S122842
46. Nasseri MA, Behravesh S, Allahresani A, Kazemnejadi M (2019) Bioresour Bioprocess 6:5. https://doi.org/10.1186/s40643-019-0240-1
47. Nasseri MA, Shahabi M, Allahresani A, Kazemnejadi M (2019) Asian J Green Chem 3:382. https://doi.org/10.22034/ajgc.2018.144365.1099
48. Rajan R, Chandran K, Harper SL, Yun SI, Kalaichelvan PT (2015) Ind Crops Prod 70:356–373. https://doi.org/10.1016/j.indcrop.2015.03.015
49. Baharara J, Namvar F, Ramezani T, Hosseini N, Mohamad R (2014) Molecules 19:4624–4634. https://doi.org/10.3390/molecules19044624
50. Khalil MM, Ismail EH, El-Baghdady KZ, Mohamed D (2014) Arab J Chem 7:1131–1139. https://doi.org/10.1016/j.arabjc.2013.04.007
51. Tripathy A, Raichur AM, Chandrasekaran N, Prathna TC, Mukherjee A (2010) J Nanopart Res 12:237–246. https://doi.org/10.1007/s11051-009-9602-5
52. Panigrahi S, Basu S, Praharaj S, Pande S, Jana S, Pal A, Ghosh SK, Pal T (2007) J Phys Chem C 111:4596–4605. https://doi.org/10.1021/jp067554u
53. Roy S, Mukherjee T, Chakraborty S, Das TK (2013) Dig J Nanomater Bios 8:197–205
54. Wrótniak-Drzewiecka W, Gaikwad S, Laskowski D, Dahm H, Niedojadło J, Gade A, Rai M (2014) Austin J Biotechnol Bioeng 1:7
55. Jyoti K, Baunthiyal M, Singh A (2016) J Radiat Res Appl Sci 9:217–227. https://doi.org/10.1016/j.jrras.2015.10.002
56. Shao Y, Jin Y, Dong S (2004) Chem Commun 9:1104–1105. https://doi.org/10.1039/B315732F
57. Prakash P, Gnanaprakasam P, Emmanuel R, Arokiyaraj S, Saravanan M (2013) Colloids Surf B Biointerfaces 108:255–259. https://doi.org/10.1016/j.colsurfb.2013.03.017
58. Herves P, Perez-Lorenzo M, Liz-Marzan LM, Dzubiella J, Lu Y, Ballauff M (2012) Chem Soc Rev 41:5577–5587. https://doi.org/10.1039/C2CS35029G
59. Devi TB, Ahmaruzzaman M, Begum S (2016) New J Chem 40:1497–1506. https://doi.org/10.1039/C5NJ02367J
60. Gu S, Wunder S, Lu Y, Ballauff M, Fenger R, Rademann K, Jaquet B, Zaccone A (2014) J Phys Chem 118:18618–18625. https://doi.org/10.1021/jp5060606
61. Narayanan KB, Park HH, Sakthivel N (2013) Spectrochim Acta Part A 116:485–490. https://doi.org/10.1016/j.saa.2013.07.066
62. Rostami-Vartooni A, Nasrollahzadeh M, Alizadeh M (2016) J Alloys Compd 680:309–314. https://doi.org/10.1016/j.jallcom.2016.04.008
63. Veisi H, Azizi S, Mohammadi P (2018) J Clean Prod 170:1536–1543. https://doi.org/10.1016/j.jclepro.2017.09.265
64. Sharma V, Ramawat KG (2013) 3 Biotech 3:11. https://doi.org/10.1007/s13205-012-0064-6
65. Alfatemi SMH, Rad JS, Rad MS, Mohsenzadeh S, da Silva JAT (2015) 3 Biotech 5:39–44. https://doi.org/10.1007/s13205-014-0197-x